Kinetic Evidence for Half-of-the-Sites Reactivity in $tRNA^{Trp}$ Aminoacylation by Tryptophanyl-tRNA Synthetase from Beef Pancreas†

Véronique Trézéguet,* Michel Merle, Jean-Claude Gandar, and Bernard Labouesse

Institut de Biochimie Cellulaire et Neurochimie, CNRS, 33077 Bordeaux Cedex, France

Received September 13, 1985; Revised Manuscript Received April 9, 1986

ABSTRACT: The aminoacylation reaction catalyzed by the dimeric tryptophanyl-tRNA synthetase from beef pancreas was studied under pre-steady-state conditions by the quenched-flow method. The transfer of tryptophan to $tRNA^{Trp}$ was monitored by using preformed enzyme–bis(tryptophanyl adenylate) complex. Combinations of either unlabeled or L-[^{14}C]tryptophan-labeled tryptophanyl adenylate and of aminoacylation incubation mixtures containing either unlabeled tryptophan or L-[^{14}C]tryptophan were used. We measured either the formation of a single labeled aminoacyl-$tRNA^{Trp}$ per enzyme subunit or the turnover of labeled aminoacyl-$tRNA^{Trp}$ synthesis. Four models were proposed to analyze the experimental data: (A) two independent and nonequivalent subunits; (B) a single active subunit (subunits presenting absolute "half-of-the-sites reactivity"); (C) alternate functioning of the subunits (flip-flop mechanism); (D) random functioning of the subunits with half-of-the-sites reactivity. The equations corresponding to the formation of labeled tryptophanyl-$tRNA^{Trp}$ under each labeling condition were derived for each model. By use of least-squares criteria, the experimental curves were fitted with the four models, and it was possible to disregard models B and C as likely mechanisms. Complementary experiments, in which there was no significant excess of ATP–Mg over the enzyme–adenylate complex, emphasized an activator effect of free L-tryptophan on the rate of aminoacylation. This result disfavored model A. Model D was in agreement with all data. The analyses showed that the transfer step was not the major limiting reaction in the overall aminoacylation process.

The synthesis of aminoacyl-tRNAs catalyzed by aminoacyl-tRNA synthetases proceeds via a two-step reaction pathway, formation of an aminoacyl adenylate followed by the transfer of the aminoacyl moiety to the specific tRNA (Mehler & Chakraburty, 1971; Schimmel & Söll, 1979). A broad understanding of these enzyme mechanisms can be obtained by determining the sequence of substrate addition and product release under steady-state conditions according to Cleland's rules (Cleland, 1963). This was applied to monomeric enzymes (Kern & Lapointe, 1981; Thiebe, 1983; Freist & Cramer, 1983) as well as to oligomeric enzymes (Penneys & Muench, 1974; Mérault et al., 1978; Thiebe, 1978). However, there are limitations to this approach. Using steady-state methods, transient enzyme complexes and intermediate steps involving conformational changes cannot be detected and the kinetic parameters of the elementary steps cannot be determined. Furthermore, for oligomeric enzymes that show Michaelian patterns, the stoichiometry of the active sites cannot be defined, nor can their equivalence or nonequivalence. For such characterizations, pre-steady-state data are necessary. Oligomeric aminoacyl-tRNA synthetases exhibit, as a general feature, binding anticooperativity toward tRNA (Pingoud et al., 1975; Akhverdyan et al., 1977; Pachmann & Zachau, 1978; Huang et al., 1982), a feature that has led to the proposal of "half-of-the-sites reactivity" for several of these enzymes (Jakes & Fersht, 1975; Mulvey & Fersht, 1978; Akhverdyan et al., 1977).

To be significant at the molecular level, the macroscopic concept of half-of-the-sites reactivity needs an accurate definition. Lazdunski (1972) has proposed the flip-flop mechanism to account for the kinetic behavior of half-site enzymes. This mechanism was considered to hold in the cases of yeast phenylalanyl-tRNA synthetase (Fasiolo et al., 1977) and of beef pancreas tryptophanyl-tRNA synthetase (Favorova et al., 1981). Direct evidence for the reliability of such a mechanism is not easy to obtain. Bale et al. (1980a) have presented a method to test the flip-flop hypothesis. This method is based on the analysis of patterns of kinetic experiments performed with alternate substrate and inhibition product under steady-state conditions. Applying their method to the study of *Escherichia coli* alkaline phosphatase, Bale et al. (1980a) concluded that this enzyme does not follow the criteria of a flip-flop mechanism, although kinetics under pre-steady-state conditions at low substrate concentration show that only one active site is reactive at any one time (Bale et al., 1980b). For aminoacyl-tRNA synthetases, the high specificity of the aminoacylation reaction precludes the use of alternate substrates in mechanistic studies under steady-state conditions; hence other approaches must be considered. For these enzymes, one approach is to use the intermediate enzyme–(aminoacyl adenylate) complex, which can be isolated in a majority of cases, to study the discrete transfer step under pre-steady-state conditions.

This work describes an attempt to use these possibilities in the case of beef tryptophanyl-tRNA synthetase, an α_2 dimeric enzyme with two sets of binding sites for its substrates (Dorizzi et al., 1977; Zinoviev et al., 1977; Graves et al., 1979, 1980). This enzyme exhibits anticooperative binding for both L-tryptophan and $tRNA^{Trp}$ (Graves et al., 1979; Akhverdyan et al., 1977) and fulfills the criteria for a ping-pong mechanism in the overall aminoacylation process (Mérault et al., 1978). The two enzyme subunits have the same catalytic efficiency in the L-tryptophan activation reaction as in the adenylate pyrophosphorolysis (Mazat et al., 1982; Merle et al., 1984).

† This work was supported by grants from the Centre National de la Recherche Scientifique, from the University of Bordeaux II, and from the Fondation de la Recherche Medicale.

0006-2960/86/0425-7125$01.50/0

The monophasic kinetics in adenylate pyrophosphorolysis suggest that the enzyme–bis(tryptophanyl adenylate) complex is symmetrical in the absence of $tRNA^{Trp}$. Under steady-state conditions, the dependence of the rate of $tRNA^{Trp}$ aminoacylation on the concentration $tRNA^{Trp}$ exhibits simple Michaelian patterns (Dorizzi et al., 1977; Mérault et al., 1978). From affinity labeling of the protein, using analogues of its reaction product (Akhverdyan et al., 1977; Favorova et al., 1981), and from a preliminary study under pre-steady-state conditions (Trézéguet et al., 1983) half-of-the-sites reactivity was proposed for the aminoacylation process.

In this study, the quenched-flow method was applied to follow the transfer of L-tryptophan from tryptophanyl adenylate to $tRNA^{Trp}$, in order to define whether both enzyme subunits were able to catalyze the transfer of L-tryptophan to the homologous tRNA and to elucidate the mechanism of the reaction. Combinations of either labeled or nonlabeled free L-tryptophan and either labeled or nonlabeled preformed enzyme–bis(tryptophanyl adenylate) complexes were used. Taking into account both the dimeric structure of the enzyme and the two-step reaction pathway (activation and transfer), simple theoretical models were proposed. The experimental data were fitted to the models by least-squares computation to elucidate the precise mechanism operating for this reaction.

Materials and Methods

Tryptophanyl-tRNA synthetase from beef pancreas was prepared according to Mérault et al. (1978); its concentration was determined by absorbance spectrophotometry ($\epsilon = 90\,000$ $M^{-1}\cdot cm^{-1}$; Lemaire et al., 1969). Beef liver $tRNA^{Trp}$ was prepared as in Fournier et al. (1976); it was checked that there was no remaining tryptophanyl-$tRNA^{Trp}$ at the end of the preparation. According to the batch used, the amino acid acceptance of $tRNA^{Trp}$ was 800 or 1500 pmol/OD_{260} absorbance unit. The molar concentration of accepting $tRNA^{Trp}$ was calculated by using these values. The purest batch of $tRNA^{Trp}$ (1500 pmol/OD) was used for fast kinetic experiments. The other batch (800 pmol/OD) was used in the experiments where no kinetic parameter was searched, as will be indicated in the legends of the figures. In all cases, $tRNA^{Trp}$ concentration was given as accepting $tRNA^{Trp}$ concentration. It was checked that both batches of tRNA gave the same rate constant of $tRNA^{Trp}$ aminoacylation under steady-state conditions, indicating that the contaminants had no effect on the overall reaction rate.

Inorganic pyrophosphatase (500 units/mg) was purchased from Sigma and L-[^{14}C]tryptophan (58 mCi/mmol) from Amersham.

The experiments were performed in 100 mM tris(hydroxymethyl)aminomethane hydrochloride (Tris-HCl) buffer, pH 8, containing 0.1 mM ethylenediaminetetraacetic acid (EDTA) and 1 mM dithioerythritol, at 25 °C. For each experimental condition, the total magnesium concentration was calculated according to O'Sullivan and Smithers (1979), using a dissociation constant of 15 μM for the ATP–Mg complex at pH 8 and 25 °C, in order to keep the free magnesium concentration, Mg^{2+}, at 1 mM. This concentration was previously shown to lead to the maximal rate constant of $tRNA^{Trp}$ aminoacylation and was used in the studies of tryptophanyl adenylate formation by tryptophanyl-tRNA synthetase from beef (Merle et al., 1984).

Preformation of the Enzyme–Bis(tryptophanyl∼AMP) Complex. Enzyme–bis(adenylate) complex was preformed in situ by incubating tryptophanyl-tRNA synthetase at 25 °C with either radioactive or nonradioactive L-tryptophan (2.5 times the enzyme concentration) and 50 μM ATP–Mg in the presence of 1 unit/mL inorganic pyrophosphatase. Under these conditions, the complex is synthesized within 1 min (Mazat et al., 1982; Merle et al., 1984).

Kinetic Studies. For reaction times above 5 s, the experiments were carried out manually. Reactions were initiated by mixing equal volumes (200 μL) of the preformed enzyme–bis(tryptophanyl adenylate) complex with the substrates at twice their final concentration. Aliquots (40 μL) were withdrawn as a function of time and spotted on dried 3MM Whatman, 2.4-cm diameter, paper disks presoaked in 5% trichloroacetic acid containing 0.5% DL-tryptophan (Nishimura & Novelli, 1964). The disks were then washed in 5% trichloroacetic acid containing 0.5% DL-tryptophan (3 × 15 min) and by ethanol (2 × 15 min) and dried. The radioactivity trapped in the paper disks was determined with a toluene scintillator solvent in an Intertechnique SL 30 counter.

Quenched-flow experiments were carried out by using equipment constructed according to Gangloff et al. (1984). The reaction was started by mixing the preformed enzyme–bis(tryptophanyl adenylate) complex and substrate solutions (0.5 mL per syringe) and was stopped at different reaction times by the addition of 1% trichloroacetic acid contained in the third syringe (1 mL). As a function of the flow rate and of the reaction chamber volume, 12 different fractions (35 μL of substrate solution, 35 μL of enzyme solution, and 70 μL of quencher solution), which corresponded to equally spaced incubation times on a 0–300-ms time scale, were flushed in a fixed-angle Teflon rotor of a microcentrifuge used as a fraction collector. A 3MM Whatman (2.4-cm diameter) paper disk, prepared as above, was disposed in the bottom of each well of the rotor, to ensure entire and rapid absorption of the solution (140-μL final volume). After a short centrifugation, the paper disks were removed and washed as above.

Data Analysis. Analysis of the formation of tryptophanyl-$tRNA^{Trp}$ as a function of time was made by comparing the data of the quenched-flow experiments to theoretical points, calculated by using the analytical expressions derived from four mechanistic models of the enzyme (see the text and the Appendix). The difference d between the theoretical and experimental values was determined for each point. The standard error along the whole curve was $S = [(\sum d^2)/(N - n)]^{1/2}$, where N was the number of experimental points and n the number of the unknown parameters. For each model, the expression of the aminoacyl-tRNA concentration as a function of time depended on the rate constants of the different steps. An iterative procedure was used to change the numerical values of these parameters until the lowest value of S was reached. The formation of tryptophanyl-$tRNA^{Trp}$ was expressed as the number of moles of labeled aminoacyl-tRNA formed per mole of preformed enzyme–bis(adenylate) complex. The values of the parameters and their standard deviations were calculated by using the jackknife method proposed by Cornish-Bowden and Wong (1978). Three sets of points were analyzed all together and by pairs, leading to the determination of the parameter values and of the corresponding standard errors for each model, as described in Merle et al. (1984). The calculations were done with a Hewlett-Packard 9845 microcomputer.

Results

Aminoacylation Reaction under Saturating Substrate Concentrations. In order to test whether or not both sites of the enzyme were active in the aminoacylation reaction, the appearance of L-[^{14}C]tryptophanyl-$tRNA^{Trp}$ was measured as a function of time from an enzyme–bis(tryptophanyl adenylate) complex. This complex was preformed either with L-

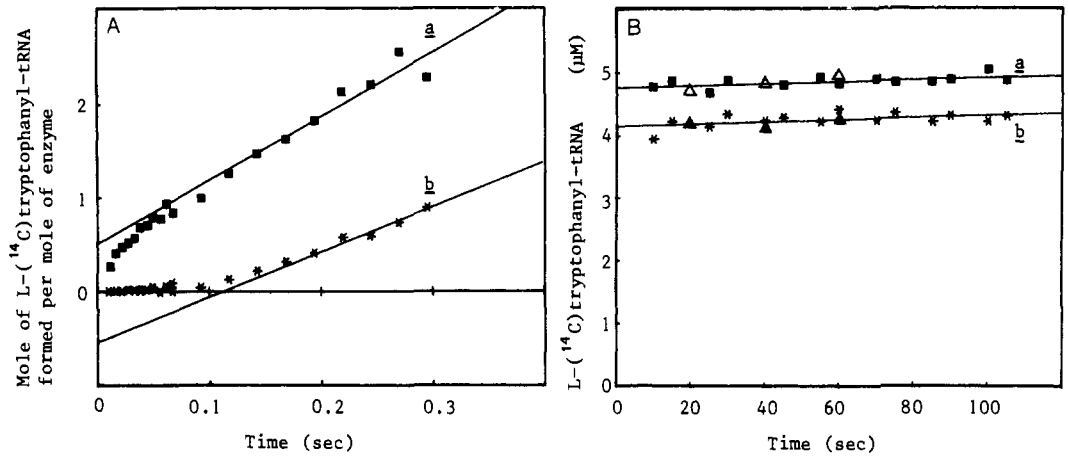

FIGURE 1: Aminoacylation reaction under saturating substrate concentrations. (A) Pre-steady-state kinetics of tRNA^{Trp} aminoacylation using preformed enzyme–bis(tryptophanyl adenylate) complexes. These experiments were done in a quenched-flow apparatus. The first syringe contained 0.5 μM tryptophanyl-tRNA synthetase, 10 mM ATP, 10 mM magnesium acetate, 1 unit/mL inorganic pyrophosphatase, and 1.25 μM L-[^{14}C]tryptophan (conditions a, ■) or unlabeled L-tryptophan (conditions b, *). These mixtures were allowed to react 5 min at 25 °C to ensure the enzyme–(tryptophanyl ~AMP) complex formation. In both cases, the second syringe contained 100 μM L-[^{14}C]tryptophan, 1.84 mM magnesium acetate, and 10 μM tRNA^{Trp} (1500 pmol/OD) and the third syringe 1% trichloroacetic acid as quenching solution. Under these conditions, the free Mg^{2+} concentration in the reaction chamber was 1 mM. (B) Charging plateau of tRNA^{Trp} under conditions of aminoacylation using preformed enzyme–bis(tryptophanyl adenylate) complexes. These complexes were preformed with 0.6 μM enzyme, 1.5 μM L-[^{14}C]tryptophan (conditions a, ■ and △) or unlabeled L-tryptophan (conditions b, * and ▲), 10 mM ATP, 10 mM magnesium acetate, and 1 unit/mL inorganic pyrophosphatase. After a 5-min incubation at 25 °C, 20 μL of these mixtures was mixed with 20 μL of a solution containing 10 μM tRNA^{Trp} (800 pmol/OD, ■ and *, or 1500 pmol/OD, △ and ▲), 1.84 mM magnesium acetate, and 100 μM L-[^{14}C]tryptophan. The free Mg^{2+} concentration after the two solutions were mixed was 1 mM. At different time intervals, 30 μL was spotted onto paper disks presoaked in a solution containing 5% trichloroacetic acid and 0.5% DL-tryptophan. The values of the extrapolations back to time zero of the straight lines were determined by linear regression. The obtained values were 4.76 ± 0.03 μM (conditions a) and 4.15 ± 0.05 μM (conditions b), respectively.

[^{14}C]tryptophan or with nonradioactive L-tryptophan, and it was rapidly mixed with an excess of L-[^{14}C]tryptophan (50 μM), ATP–Mg (5 mM), and tRNA^{Trp} (5 μM) (final concentrations). At 25 °C, these concentrations ensure a maximal steady-state aminoacylation rate constant [6.5 s^{-1} per dimer (Mérault et al., 1978)]. The pre-steady-state phase of the reaction was studied on a 0–300-ms time scale by using a quenched-flow apparatus (Figure 1A), whereas the plateau of tRNA aminoacylation was measured on a 20–110-s time scale (Figure 1B).

Formation of L-[^{14}C]tryptophanyl-tRNA^{Trp} reached the charging plateau (5 μM) when the reaction was carried out with a radioactive preformed enzyme–bis(tryptophanyl adenylate) complex (Figure 1B, conditions a) and did not when the experiment was performed with a nonradioactive preformed enzyme–bis(tryptophanyl adenylate) complex (Figure 1B, conditions b). The difference between the two plateaus of radioactive aminoacyl-tRNA synthesis was 0.61 ± 0.08 μM, with an enzyme–bis(tryptophanyl adenylate) complex concentration of 0.3 μM in both cases. This result indicated that 2.04 ± 0.28 mol of radioactive L-tryptophanyl-tRNA per mole of dimer was synthesized under conditions a, in addition to what was synthesized under conditions b. Therefore, both sites of the enzyme were able to catalyze the transfer reaction.

As shown in Figure 1A, when the tryptophanyl adenylates were preformed with labeled L-tryptophan, the formation of L-[^{14}C]tryptophanyl-tRNA^{Trp} was characterized by a burst followed by a linear phase of aminoacylation. This burst indicated that the charging reaction occurred in at least two steps and that the first one (transfer of L-tryptophan to tRNA^{Trp}) was not rate-determining. When the tryptophanyl adenylates were preformed with nonradioactive L-tryptophan (Figure 1A, curve b), the first phase was a lag phase and preceded the formation of labeled L-tryptophanyl-tRNA^{Trp}, indicating that at least 1 mol of unlabeled aminoacyl-tRNA^{Trp} per enzyme was synthesized during the first reaction period. The slope of the apparent linear phase under conditions a of Figure 1A (k = 6.8 s^{-1}) was consistent with the known value of the aminoacylation rate constant under steady-state conditions (6.5 s^{-1}), indicating that the aminoacylation steady state was reached within the 0–300-ms time scale. The slope of the apparent final straight line under conditions b (k' = 4.8 s^{-1}) was smaller, indicating that the steady state of radioactive aminoacyl-tRNA synthesis was not yet reached under these conditions during that time scale.

First Aminoacylation Cycle of the Enzyme under Saturating Substrate Concentrations. The first enzyme aminoacylation cycle under saturating substrate concentrations was studied by mixing 0.5 μM of the preformed enzyme–(L-[^{14}C]tryptophanyl adenylate) complex with 5 mM ATP–Mg, 50 μM unlabeled L-tryptophan, and 5 μM tRNA^{Trp} (final concentrations) in the quenched-flow apparatus. Under these conditions, the transfer of only one L-tryptophan molecule per subunit from the preformed tryptophanyl adenylates could result in the formation of radioactive aminoacyl-tRNA. Figure 2A (curve a) shows that the appearance of the labeled product was biphasic. The first process had a rate constant of 26 s^{-1} and an amplitude of 1 mol of aminoacyl-tRNA formed per mole of enzyme. The second process had a rate constant on the order of 3 s^{-1} (calculated from the second part of the curve on the 300-ms time scale). The maximal extent of labeled L-tryptophanyl-tRNA^{Trp} formation on a longer time scale was measured under the same experimental conditions as mentioned above. Figure 2B, curve a, shows that approximately 2 mol of radioactive aminoacyl-tRNA^{Trp} per mole of enzyme was synthesized within the first few seconds. Therefore, the second process of curve a (Figure 2A) had also an amplitude of 1 mol of L-tryptophan transferred per mole of enzyme. Under these conditions (50 μM unlabeled L-tryptophan, 5 mM ATP–Mg, and 5 μM tRNA^{Trp}), all the tRNA^{Trp} was aminoacylated, as shown in Figure 1B. The labeled product synthesized during the early reaction time from the preformed radioactive tryptophanyl adenylates remained stable within the 20–300-s time scale (Figure 2B, conditions a). These

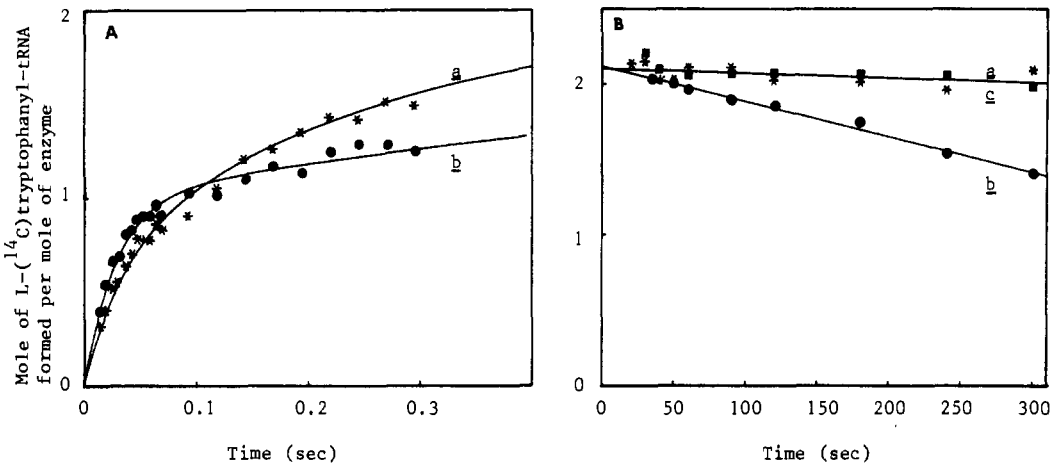

FIGURE 2: (A) Pre-steady-state kinetics of the aminoacylation reaction from a preformed enzyme–bis(tryptophanyl adenylate) complex under limiting and nonlimiting substrate concentrations. The first syringe of the quenched-flow apparatus contained 0.5 μM synthetase, 1.25 μM L-[^{14}C]tryptophan, 50 μM ATP, 1.03 mM magnesium acetate, and 1 unit/mL inorganic pyrophosphatase. This solution was incubated 5 min at 25 °C to allow the complex formation. The second syringe contained either 10 μM tRNA^{Trp} (1500 pmol/OD), 100 μM unlabeled L-tryptophan, 10 mM ATP, and 10.8 mM magnesium acetate (conditions a, *) or 1.03 mM magnesium acetate and 10 μM tRNA^{Trp} (1500 pmol/OD) (conditions b, ●). The quencher was 1% trichloroacetic acid. (B) Effect of the presence of small ligands on the charging plateaus of tRNA^{Trp}. The enzyme–bis(tryptophanyl adenylate) complex was preformed by incubating 5 min at 25 °C a solution containing 0.6 μM enzyme, 1.5 μM L-[^{14}C]tryptophan, 50 μM ATP, 1.03 mM magnesium acetate, and 1 unit/mL inorganic pyrophosphatase. A 200-μL aliquot of this solution was then mixed with 200 μL of a solution containing either 10 μM tRNA^{Trp}, 100 μM unlabeled tryptophan, 10.8 mM magnesium acetate, and 10 mM ATP (conditions a, *) or 10 μM tRNA and 1.03 mM magnesium acetate (conditions b, ●) or 10 μM tRNA^{Trp}, 1.03 mM magnesium acetate, and 100 μM unlabeled L-tryptophan (conditions c, ■). At different time intervals, aliquots (40 μL) were spotted onto paper disks presoaked in a solution containing 5% trichloroacetic acid and 0.5% DL-tryptophan. In every condition, the extrapolation back to time zero of the straight line was 2.1 mol of L-[^{14}C]Trp-tRNA^{Trp} per mole of enzyme. Under all experimental conditions in both (A) and (B), the free Mg^{2+} concentration was 1 mM.

observations were consistent with the difference of 2 mol of aminoacyl-tRNA per mole of enzyme between curves a and b of Figure 1B.

These data indicated that the rates of synthesis of tryptophanyl-tRNAs from the two preformed tryptophanyl adenylates were different. Two kinds of enzyme behavior could therefore account for these findings: (i) both subunits of the enzyme could catalyze simultaneously the transfer of two molecules of L-tryptophan, but through independent ways and with different rate constants; (ii) only one subunit was functional at a time (half-of-the-sites reactivity), and as a consequence of interactions between the two subunits, the dimer catalyzed the transfer of only one molecule of L-tryptophan per catalytic cycle.

First Aminoacylation Cycle of the Enzyme under Limiting Substrate Concentrations. To study the behavior of the two subunits through the first enzyme catalytic cycle only, the aminoacylation reaction was followed under limiting concentrations of small substrates, starting from a preformed enzyme–bis(L-[^{14}C]tryptophanyl adenylate) complex (0.25 μM final concentration). The concentrations of free L-tryptophan (0.12 μM) and free ATP–Mg (25 μM) corresponded to the excess remaining after the tryptophanyl adenylate preformation; they were small as compared to the values of the dissociation constants of tryptophan and ATP (K_1^{Trp} = 1.6 μM, K_2^{Trp} = 18.5 μM, and K^{ATP} = 1.4 mM; Merle et al., 1984). Under these conditions, at most only one catalytic cycle per subunit could occur. At time zero, this complex was mixed with an excess of tRNA^{Trp} (5 μM final concentration) in the quenched-flow machine. The formation of L-[^{14}C]tryptophanyl-tRNA as a function of time is shown in Figure 2A, curve b. As under conditions a, the reaction was biphasic within the 0–300-ms time scale. However, the behavior of the enzyme was different from that observed under conditions a. The first process was faster and had a rate constant of 35 s^{-1} (with an amplitude of 1 mol of aminoacyl-tRNA synthesized per mole of enzyme). The second process was slower and had a rate constant of 1 s^{-1} (calculated from the slope of the second part of the curve).

The rate constants obtained under conditions b, Figure 2A, were compared to those obtained for the first catalytic cycle under nearly saturating substrate concentrations (conditions a, Figure 2A). The rates of both phases were modified, but in opposite ways: high concentrations of the small ligands slowed down the first phase (26 s^{-1} instead of 35 s^{-1}) and accelerated the second phase (3 s^{-1} instead of 1 s^{-1}). The same activating effect on the second phase was observed when the reaction was carried out at high tryptophan and low ATP–Mg concentrations whereas no activating effect was observed at low tryptophan and high ATP–Mg concentrations (data not shown). These findings indicated that the increase of the rate constant of the second phase was only related to the excess of tryptophan.

The observation was continued on a longer time scale. Figure 2B, curve b, shows the variation of tryptophanyl-tRNA concentration between 20 and 300 s. The decrease of labeled aminoacyl-tRNA concentration corresponded to the enzymatic hydrolysis of the product formed during the initial period of the reaction. As under conditions a, the extrapolation back to time zero of curve b corresponded to 2.1 ± 0.11 mol of labeled L-tryptophanyl-tRNA^{Trp} synthesized per mole of synthetase. This finding confirmed that both catalytic centers of the enzyme had been productive.

Effect of L-Tryptophan on Enzyme-Catalyzed Aminoacyl-tRNA Hydrolysis. The variation of L-[^{14}C]tryptophanyl-tRNA^{Trp} concentration was studied as a function of time when the radioactive preformed enzyme–bis(tryptophanyl adenylate) complex (0.3 μM) was mixed with 5 μM tRNA^{Trp} and 50 μM L-tryptophan (final concentrations) at low (25 μM) ATP–Mg concentration (Figure 2B, curve c). The rate of aminoacyl-tRNA hydrolysis was slowed down as compared to that observed in the absence of added L-tryptophan (Figure 2B, curve b) and was the same as the rate in the presence of both ATP–Mg and L-tryptophan at nearly saturating con-

Scheme I

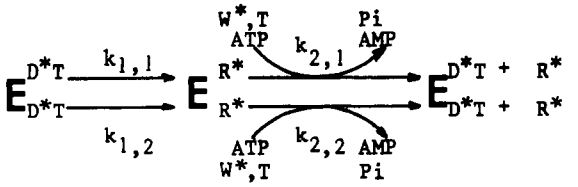

centrations (Figure 2B, curve a). Because of the large isotopic dilution of free L-[^{14}C]tryptophan, this result could not be explained by an enzymatic turnover of tRNA aminoacylation but indicated a protective effect of L-tryptophan against the enzymatic hydrolysis of aminoacyl-tRNA. This strong inhibition of the aminoacyl-tRNA hydrolysis by the amino acid suggested that L-tryptophan and L-tryptophanyl-tRNA^{Trp} were competing for binding to the enzyme.

Analysis of the Pre-Steady-State Phase of tRNA^{Trp} Aminoacylation under Saturating Substrate Concentrations. Theoretical Models. To interpret the pre-steady-state phase of tRNA^{Trp} aminoacylation, the rapid-mixing experiments were submitted to a more detailed analysis. Taking into account the dimeric structure of tryptophanyl-tRNA synthetase, we postulated four simple theoretical models for the aminoacylation mechanism, which could lead to the results of Figures 1A, curves a and b, and 2A, curve a. The substrate concentrations used in these experiments (50 μM L-tryptophan and 5 mM ATP–Mg) were considered as saturating the enzyme under rapid equilibrium. The concentration of tRNA^{Trp} was 5 μM and was regarded as saturating at least one site of the synthetase [K_m = 0.26 μM (Dorizzi et al., 1977)]. The substrate concentrations were much higher than the enzyme concentration and were considered as being constant during the aminoacylation pre-steady-state phase.

These models took into account a two-step reaction pathway for each catalytic site. According to each model, the analytical expression of radioactive aminoacyl-tRNA concentration as a function of time was derived (detailed calculations are given in the Appendix). In the following models, E corresponds to the enzyme, W to L-tryptophan, D to tryptophanyl adenylate, T to tRNA^{Trp}, and R to L-tryptophanyl-tRNA^{Trp}. The asterisk indicates L-[^{14}C]tryptophan-containing derivatives: tryptophan, tryptophanyl adenylate, or aminoacyl-tRNA. [E_0] is the total enzyme concentration.

Model A: Two Independent and Nonequivalent Subunits. In this model, the two subunits are considered as independent and nonequivalent; they are able to carry out the aminoacylation reaction simultaneously. The asymmetrical behavior is related to different rates of catalysis by the two subunits. The difference between the rate constants of the transfer steps reflects either an intrinsic difference in catalytic efficiency of the two active centers or anticooperative binding of tRNA^{Trp} (or both). Different rate constants for the second step are a consequence of an asymmetrical behavior in the processes following the transfer step.

In the case of radioactive preformed adenylates (Figure 1A, conditions a), the model is depicted in Scheme I. $k_{1,i}$ (i = 1 or 2) refers to the rate constant of the transfer step on subunit i and $k_{2,i}$ to the overall rate constant of all the processes following the transfer (including tryptophan activation, tryptophanyl-tRNA dissociation from site i, and any isomerization process). The corresponding expression of total labeled aminoacyl-tRNA concentration (free and bound to the enzyme) as a function of time, $[R^*]_1$, is shown by eq 1 which is given by integration of the rate equations (see the Appendix).

$$[R^*]_1 = \sum_{i=1}^{i=2} \frac{k_{1,i}[E_0]}{k_{1,i} + k_{2,i}} \left[\frac{k_{1,i}}{k_{1,i} + k_{2,i}} [1 - e^{-(k_{1,i}+k_{2,i})t}] + k_{2,i}t \right] \quad (1)$$

In the case of nonradioactive preformed adenylates, Figure 1A (curve b), the reaction pathway is depicted in Scheme II.

Equation 2 expresses labeled tryptophanyl-tRNA^{Trp} concentration, $[R^*]_2$, as a function of time.

$$[R^*]_2 = \sum_{i=1}^{i=2} [E_0] \left[\frac{k_{1,i}k_{2,i}t}{k_{1,i} + k_{2,i}} + \frac{k_{1,i}^2}{(k_{1,i} + k_{2,i})^2} [1 - e^{-(k_{1,i}+k_{2,i})t}] + e^{-k_{1,i}t} - 1 \right] \quad (2)$$

Model B: Absolute Half-of-the-Sites Reactivity. Only one subunit of the dimer, always the same, leads to the transfer reaction. This implies an asymmetrical enzyme–bis(tryptophanyl adenylate) complex toward the binding of tRNA^{Trp} (strong anticooperativity). Although the results of the experiments described in Figure 1B and in Figure 2B (curve a) demonstrated that such a mechanism could be excluded, the analysis was carried out as an indication of the reliability of the analytical method used.

Scheme III depicts the reaction in the case of labeled preformed adenylates. k_1 refers to the transfer step and k_2 to all other steps. The analytical expression of labeled aminoacyl-tRNA as a function of time, $[R^*]_3$, is given by

$$[R^*]_3 = \frac{k_1[E_0]}{k_1 + k_2} \left[\frac{k_1}{k_1 + k_2} [1 - e^{-(k_1+k_2)t}] + k_2 t \right] \quad (3)$$

In the case of unlabeled preformed adenylates, the reaction can be described as in Scheme IV.

The corresponding expression of the concentration of radioactive tryptophanyl-tRNA as a function of time, $[R^*]_4$, is given by

$$[R^*]_4 = [E_0] \left[\frac{k_1k_2t}{k_1 + k_2} + \frac{k_1^2}{(k_1 + k_2)^2} [1 - e^{-(k_1+k_2)t}] + e^{-k_1t} - 1 \right] \quad (4)$$

Model C: Flip-Flop Mechanism. Both subunits are catalytically active in the aminoacylation reaction but in an alternate way for the transfer step, thus leading to an apparent half-of-the-sites reactivity. Only one molecule of tRNA^{Trp} binds to the enzyme–bis(tryptophanyl adenylate) complex in

Scheme II

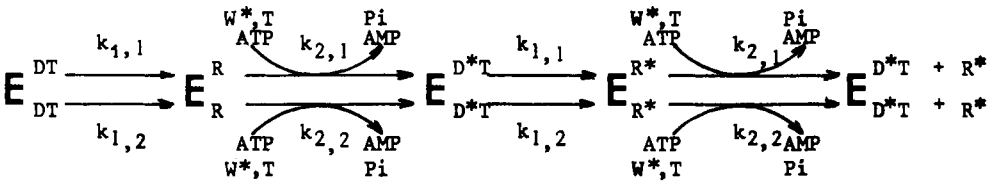

Scheme III

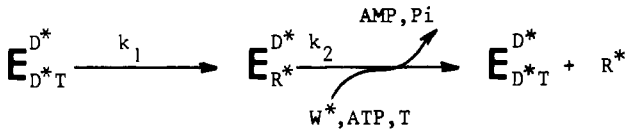

a productive way. This model implies that, for the second catalytic cycle, the fixation of a tRNA molecule on the second site occurs in the same time as or precedes a new activation process on the other catalytic center (on which one molecule of aminoacyl-tRNA was synthesized during the first catalytic cycle). The transfer step generates an asymmetrical enzyme–(tryptophanyl adenylate)–(Trp-tRNA^{Trp}) complex for the binding of tRNA. The enzyme–tRNA^{Trp} association takes place on the subunit bearing the available adenylate.

In the case of a radioactive preformed enzyme–bis(tryptophanyl adenylate) complex, the reaction pathway corresponds to Scheme V.

In this system, the expression of the concentration of labeled Trp-tRNA^{Trp} as a function of time, under conditions of labeled preformed tryptophanyl adenylates, is the same as in model B (eq 3).

In the case of nonradioactive preformed tryptophanyl adenylates, the reaction pathway can be represented by Scheme VI.

The analytical expression of radioactive aminoacyl-tRNA formed as a function of time in this latter case is $[R^*]_5$, given by

$$[R^*]_5 = [E_0]\left[-\frac{k_1^2}{(k_1+k_2)^2}e^{-(k_1+k_2)t} + \frac{k_1^2+2k_2^2-4k_1k_2}{(k_2-k_1)^2}e^{-k_1t} + \frac{k_1^2}{(k_2-k_1)^2}e^{-k_2t} + \frac{k_1k_2t}{k_2-k_1}e^{-k_1t} + \frac{k_1k_2t}{k_1+k_2} + \frac{k_1^2}{(k_1+k_2)^2} - 2\right] \quad (5)$$

Model D: Random Mechanism. In this fourth case, we have considered a random functioning of both sites under half-of-the-sites reactivity and a productive binding of only one molecule of tRNA^{Trp}. The dimer has to be symmetrical toward the binding of tRNA^{Trp}, in such a way that, after each catalytic cycle, the transfer step can occur on any of the two subunits. The dissociation of the aminoacyl-tRNA formed in a first stage on one subunit, the fixation of a new molecule of L-tryptophan and of ATP–Mg, and eventually, the activation step on that same subunit precede the binding of another molecule of tRNA^{Trp} on the dimer. Depending on the use of labeled or unlabeled preformed adenylates, this model is depicted by Schemes VII and VIII, respectively.

The analytical expressions of the formation of labeled aminoacyl-tRNA as a function of time are $[R^*]_3$ and $[R^*]_6$, given by eq 3 and 6, respectively

$$[R^*]_6 = [E_0]\left[-\frac{k_1}{V}\left[\frac{r_1+k_2}{r_1}e^{r_1t} - \frac{r_2+k_2}{r_2}e^{r_2t}\right] - \frac{k_1^2}{(k_1+k_2)^2}e^{-(k_1+k_2)t} + \frac{k_1k_2t}{k_1+k_2} - \frac{k_1^2+4k_1k_2+2k_2^2}{(k_1+k_2)^2}\right] \quad (6)$$

with

$$V = (k_1^2+k_2^2)^{1/2}$$

$$r_1 = [-(k_1+k_2)+V]/2 \qquad r_2 = [-(k_1+k_2)-V]/2$$

For each model the analytical expression of labeled aminoacyl-tRNA concentration formed under conditions a of Figure 2A is expressed by the difference between the concentration of labeled acyl-tRNA obtained under conditions a of Figure 1A minus the concentration of labeled acyl-tRNA obtained under conditions b of Figure 1A ($[R^*]_1 - [R^*]_2$, $[R^*]_3 - [R^*]_4$, $[R^*]_3 - [R^*]_5$, and $[R^*]_3 - [R^*]_6$ for models A, B, C, and D, respectively).

Results of Analysis. Using the analytical expressions thus defined for labeled aminoacyl-tRNA formation, we analyzed the experimental points obtained under conditions a and b of Figure 1A and under conditions a of Figure 2A for each theoretical case. Using "least-squares" criteria, we used an iterative procedure to search the values of the rate constants that best fitted the experimental points. The three curves were analyzed either all together or in pairs, in order to define the value and the confidence limit of the parameters by the jackknife method (see Materials and Methods). The rate constants and the standard errors corresponding to the best fit for each set of data and each model are given in Tables I and II, respectively. The curves of Figure 3 are plotted with the rate constants obtained by the jackknife procedure.

Taking the values of the standard errors (S) calculated when the three curves were fit all together as a criterion to discriminate between the four models (Table II), it appeared that the smallest S value corresponded to model D (S = 0.065). A slightly greater S value was obtained for model A (S = 0.075) whereas much larger S values were obtained for models B and C (S = 0.217 and 0.135, respectively). The comparison of standard errors resulting from individual analysis of each curve (1, 2, and 3 in Table II) led to similar conclusions. As expected, these findings showed that model B could not de-

Scheme IV

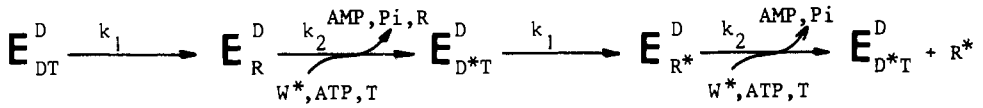

Scheme V

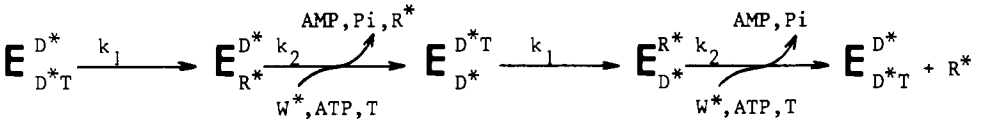

Scheme VI

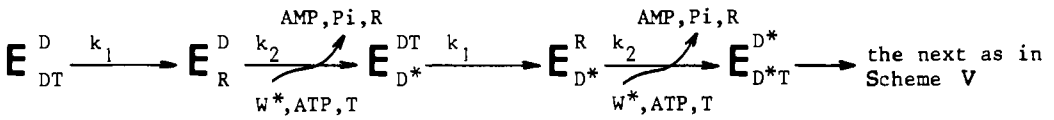

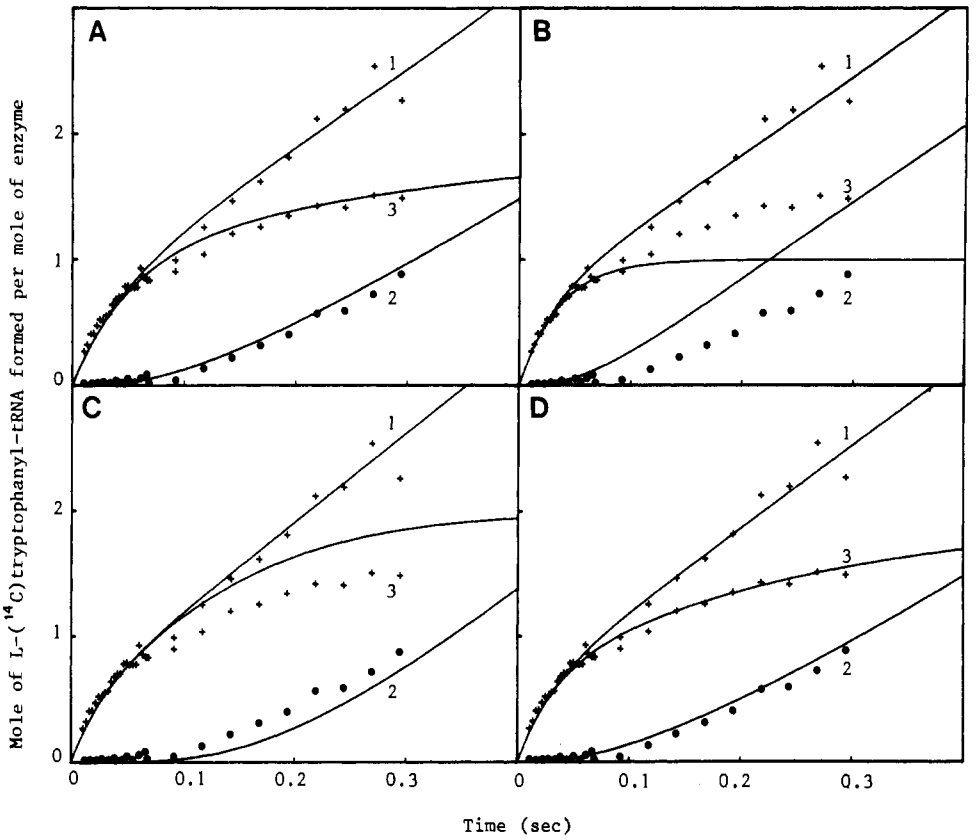

FIGURE 3: Theoretical curves corresponding to the different tested models. The sets of experimental points 1, 2, and 3 correspond to those shown in Figure 1A, curves a and b, and in Figure 2A, curve a, respectively. For each model, the theoretical curves were plotted with the final values of the parameters shown in Table I. Panels A, B, C, and D correspond to the best fits obtained with models A, B, C, and D, respectively.

Table I: Analysis of the Pre-Steady-State Phase of Aminoacylation under Saturating Substrate Concentrations[a]

model	parameter (s^{-1})	sets of experiments 1 + 2 + 3	1 + 2	1 + 3	2 + 3	final value (s^{-1})
A	$k_{1,1}$	19.1	17.5	19.8	20.2	19.1 ± 3.1
	$k_{2,1}$	4.7	4.4	5.5	4.2	4.9 ± 1.3
	$k_{1,2}$	2.5	3.1	2.2	2.2	2.7 ± 0.9
	$k_{2,2}$	17.3	15.4	20.2	19.2	17.5 ± 5.4
	k_s	6.0	6.1	6.3	5.5	6.0 ± 0.9
B	k_1	27.1	25.2	26.4	28.8	27.8 ± 3.6
	k_2	6.1	6.5	8.6	3.9	8.0 ± 6.4
	k_s	5.0	5.1	6.5	3.4	6.1 ± 4.0
C	k_1	22.4	23.3	23.4	19.4	23.9 ± 1.5
	k_2	10.1	10.6	8.4	12.4	10.1 ± 4.0
	k_s	6.9	7.3	6.2	7.7	6.9 ± 1.5
D	k_1	24.7	24.0	24.8	25.5	24.8 ± 1.5
	k_2	8.7	9.0	9.0	7.8	9.0 ± 1.5
	k_s	6.4	6.5	6.6	6.0	6.6 ± 0.7

[a] Three sets of experimental data were analyzed: set 1 corresponded to the points of Figure 1A, conditions a, set 2 to those of Figure 1A, conditions b, and set 3 to those of Figure 2A, conditions a. The analyses were performed by using either two or three sets of data in order to calculate the values of the rate constants and the standard errors with the jackknife method (Cornish-Bowden & Wong, 1978). The values given for the kinetic parameters correspond to the best fit for each tested model (A–D). k_s represents the aminoacylation rate constant under steady-state conditions, calculated with the values of the kinetic parameters.

Scheme VII

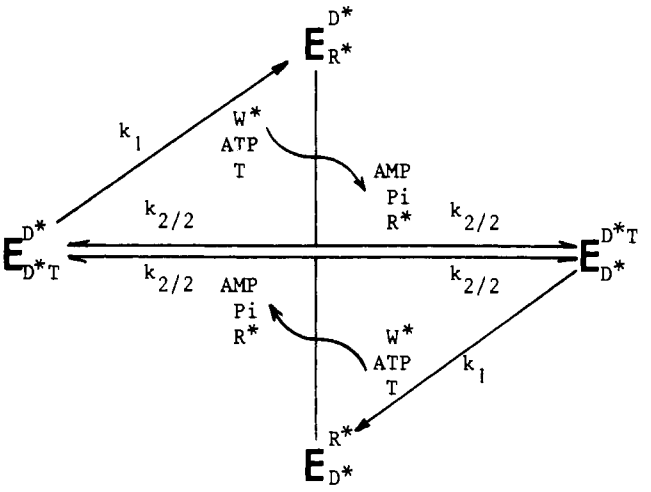

Table II: Values of Standard Errors for Each Model[a]

model	standard error for curve 1	2	3	1 + 2 + 3
A	0.108	0.053	0.072	0.075
B	0.106	0.160	0.242	0.217
C	0.101	0.098	0.196	0.135
D	0.095	0.051	0.047	0.065

[a] Standard error was equal to $[(\sum d^2)/(N - n)]^{1/2}$, with d equal to the difference between theoretical and experimental points and n equal to the number of parameters. Standard error was calculated for each of the three experimental curves and for the three experimental curves altogether, with the final values given in Table I. Curves 1–3 are defined as in Table I and Figure 3.

scribe the kinetics of the enzyme mechanism. Models A and D fitted the experimental data better than model C. Rate constants of individual steps were slightly better defined for model D than for model A. It was observed that the determination of k_1 was more accurate than that of k_2 for models B–D (Table I). This is explained by considering the first transfer step as being complete within the time scale used and well described through the first phase of the biphasic kinetics (burst and lag phases of Figure 1A and first phase of Figure 2A, curve a) while k_2 was essentially defined through the

Scheme VIII

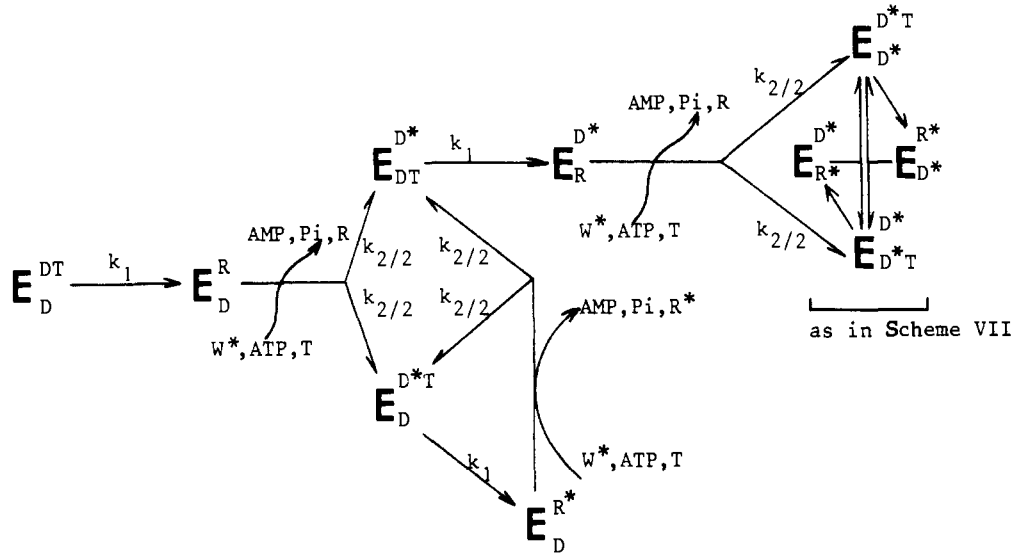

second phase, which corresponded to the steady-state settlement. In the case of model A, similar considerations could justify that the rapid-transfer rate constant $k_{1,1}$ was more accurately determined than the slow-transfer rate constant ($k_{1,2}$). The rate constant $k_{2,2}$ could not be determined with accuracy since this second step was preceded by a rate-limiting step ($k_{1,2} < k_{2,2}$).

On the basis of these analyses, we concluded that models A and D are likely possibilities describing the kinetics of the tryptophanyl-tRNA synthetase mechanism.

Discussion

Under favorable conditions of pH and temperature (pH 6.0, 4 °C), both subunits of beef tryptophanyl-tRNA synthetase are able to bind $tRNA^{Trp}$ (Dorizzi et al., 1977). This binding is anticooperative [K_d's of 36 nM and 0.9 μM for the two tRNA molecules, respectively, at pH 5.8 and 4 °C (Akhverdyan et al., 1977)]. However, under the pH and temperature conditions used in the present study (pH 8.0, 25 °C), the overall aminoacylation process is Michaelian (Mérault et al., 1978). Furthermore, at 5 μM $tRNA^{Trp}$, a concentration leading to the maximum rate of steady-state aminoacylation, a single tRNA molecule is found to bind to the enzyme as evidenced by ultracentrifugation studies (Fournier and Labouesse, unpublished data). These observations raise two questions: (1) Are both subunits able to carry out the aminoacylation reaction under these pH and temperature conditions? (2) Is there such an anticooperative binding that a single tRNA molecule is bound and aminoacylated at a time?

Both Subunits of Tryptophanyl-tRNA Synthetase Are Active in the Tryptophan Transfer Process. Figures 1B and 2B indicate that the two tryptophan molecules of a preformed enzyme–bis(tryptophanyl adenylate) complex can be transferred to $tRNA^{Trp}$. These data strongly suggest that both subunits are active in the transfer reaction. However, such a result could be theoretically obtained with a single active subunit, providing the adenylate dissociates from the unproductive subunit and reassociates to the productive one. This is an unlikely possibility because the affinity of the adenylate is very high in the case of beef tryptophanyl-tRNA synthetase [$k_d \ll 4$ nM (Iborra et al., 1973)]. Even at a high rate of association of tryptophanyl adenylate to the enzyme, such as 10^8 M^{-1} s^{-1} (Hammes & Schimmel, 1970), and considering a dissociation constant of the order of 1 nM, the rate of dissociation of the adenylate would be around 0.1 s^{-1}, at least 1 order of magnitude lower than the observed rate of aminoacylation of the second tRNA molecule (1 s^{-1} in Figure 2A, curve b).

An absolute half-of-the-sites reactivity, in which only one tryptophan could be transferred (model B), is also ruled out both by the data presented in Figures 1B and 2B and by the analysis of Table II. Therefore, it can be concluded that both subunits transfer tryptophan to $tRNA^{Trp}$.

The Subunits Do Not Transfer Tryptophan Simultaneously. The two molecules of tryptophanyl adenylate in the enzyme–bis(tryptophanyl adenylate) complex are equivalent toward pyrophosphate in the pyrophosphorolysis reaction (Mazat et al., 1982), suggesting that the dimeric enzyme–bis(tryptophanyl adenylate) complex is symmetrical. However, the biphasic kinetics of tryptophan transfer shown in Figure 2A, curve a or b, exclude the possibility that both subunits are equivalent in the form of an enzyme–bis(tryptophanyl adenylate)–bis(tRNA) complex at 5 μM $tRNA^{Trp}$. Therefore, several possibilities must be considered to explain this behavior: (i) The enzyme follows the criteria of a flip-flop mechanism (model C). This model considers that each subunit operates in turn. However, it did not allow a good fit of the three experimental curves with the same set of parameters, as shown in Figure 3, and particularly, the standard error for curve 3 of Figure 3 was around 4 times higher with model C than with model D (Table II). (ii) The two sites are independent and nonequivalent (model A). Such a mechanism would be the consequence of either anticooperative $tRNA^{Trp}$ binding or of nonidentity of the rate constants of tryptophan transfer (or both). The analyses given in Tables I and II indicate that this model could account for the data shown in Figure 1A, curves a and b, and Figure 2A, curve a. However, this model is unfavorable for the following reasons: (a) Under the experimental conditions of Figure 2A, the transfer of a single L-[^{14}C]tryptophan molecule per subunit was carried out and there was no turnover of labeled aminoacyl-tRNA synthesis. Considering independent subunits, the activatory effect on the second transfer phase promoted by adding free tryptophan could not be explained except when the binding of a second tryptophan molecule on the subunit bearing the available labeled tryptophanyl adenylate was assumed. This second tryptophan would help the proper binding of tRNA or increase the transfer rate constant. However, such an assumption implies at least three tryptophan binding sites on the dimer. Binding of a third tryptophan to the enzyme was never ob-

served (Graves et al., 1979). (b) Table I shows that, in model A, the transfer rate constant on one site ($k_{1,1}$) would be around 7-fold larger than that on the other site ($k_{1,2}$). Considering the hypothesis of a strong anticooperativity between the two tRNA binding sites, this difference should result from a poor affinity of tRNA for the second site. This should lead to a larger steady-state activity at much higher tRNA concentration than at that presently used and to a non-Michaelian pattern. This was not the case since the concentration (5 μM) of tRNA used in this study corresponded to the concentration giving the maximum activity of aminoacylation, and a Michaelian pattern was observed (Mérault et al., 1978). (c) Considering the hypothesis that the two subunits would present different rate constants, the observed Michaelian kinetics would imply the same K_m value for both sites (K_m = 0.26 μM). However, the binding of two tRNA^{Trp} at 5 μM tRNA would conflict with the finding of only 1 mol of tRNA bound per mole of synthetase at 5 μM tRNA (Fournier and Labouesse, unpublished data). (d) Model A implies that both subunits are able to catalyze simultaneously the transfer of tryptophan. This is contradictory to the findings of Akhverdyan et al. (1977) that binding covalently one molecule of a tryptophanyl-tRNA analogue to the dimer prevents both subunits from being active in the aminoacylation reaction. Consequently, it is likely that, as long as one subunit bears the aminoacyl-tRNA, the second subunit cannot operate a transfer reaction.

These different evaluations all converge to suggest that model D, which is not rejected by any of the data, holds better than model A to explain the observed kinetics of tryptophanyl-tRNA synthetase.

The Subunits Work Alternately at Random. Having concluded and taking into account that model D is the most probable reaction scheme, we can enumerate the following features of this model: (i) the enzyme–bis(adenylate) complex is symmetrical, and tRNA^{Trp} can bind to any one of the two subunits; (ii) the binding of one tRNA molecule prevents a second tRNA molecule from binding (at least in a productive way) to the second subunit; (iii) the reaction product, tryptophanyl-tRNA^{Trp}, has to depart before a second transfer cycle can start. While tryptophanyl-tRNA^{Trp} dissociates, a new binding of ATP–Mg and L-tryptophan occurs and a new activation step proceeds; (iv) as soon as the aminoacyl-tRNA has left, the enzyme–bis(tryptophanyl adenylate) complex is again symmetrical and a new tRNA^{Trp} can bind to either of the two subunits to start a new transfer reaction. It ignores which subunit was previously working; and half-of-the-sites reactivity is reached through equivalent subunits. Table I shows that the transfer step (k_1) is not the major limiting step in the steady-state process (as characterized by k_s). The rate constant k_2 is a composite of at least two different steps, tryptophanyl-tRNA release and tryptophanyl adenylate synthesis. The determinations of the individual rate constants of these two steps need further investigations.

Effect of Tryptophan and ATP on the Aminoacylation Reaction. Tryptophanyl-tRNA^{Trp} is a competitive inhibitor of tryptophan toward tRNA^{Trp} aminoacylation (Mérault et al., 1978). This accounts for the inhibitory effect of L-tryptophan upon the enzymatic hydrolysis of tryptophanyl-tRNA. Considering the aminoacylation reaction, the presence of a high concentration of L-tryptophan should prevent the binding of tryptophanyl-tRNA to the enzyme, while in the absence of L-tryptophan it should reassociate to the enzyme and inhibit the reaction. The consequence of this competition would be an apparent acceleration of the transfer step when a high tryptophan concentration is added, which is in fact what is observed (Figure 2A, second phase of curves a and b).

ATP competes with tRNA^{Trp} for binding to the enzyme, and apart from providing the chemical energy of the activation reaction, it is also a substrate able to accept tryptophan to lead to tryptophanyl-ATP ester formation in the absence of tRNA^{Trp} (Weiss et al., 1959). This competitive inhibition is illustrated by the slight decrease in the rate of the transfer step when one goes from low to high ATP concentrations (Figure 2A, curves a and b, respectively).

The method used in this study relied on the formation of an intermediate enzyme–product complex that could be isolated after different labeling conditions. Given an oligomeric enzyme featuring in a multistep mechanism and leading to such an intermediate complex, the analysis of experimental data resulting from a set of different labeling conditions may similarly lead to the determination of the number of active sites per enzyme molecule and to the most probable mechanistic model.

ACKNOWLEDGMENTS

We are grateful to Dr. Saraswasti Patel for careful reading of the manuscript.

APPENDIX

Calculation of the analytical expressions of the concentration of total radioactive aminoacyl-tRNA (free + bound) as a function of time according to the four catalytic models is given below.

Model A. In the case of radioactive preformed adenylates, model A can be depicted by the simpler scheme (I), where i

$$Ai \xrightarrow{k_{1,i}} Bi \xrightarrow{k_{2,i}} Ai + Ri \qquad \text{(I)}$$

= 1 or 2 (i refers to the ith site of the enzyme). As the two sites are independent in this model, only one will be considered for the mathematical development.

For the ith site, the total radioactive aminoacyl-tRNA concentration is $[R_T i] = [Bi] + [Ri]$. The rate equation for complex $[Bi]$ is expressed by

$$d[Bi]/dt = k_{1,i}[Ai] - k_{2,i}[Bi] \qquad \text{(1a)}$$

Using the conservation equation $[E_0 i] = [Ai] + [Bi]$, with $[E_0 i]$ = total ith site concentration, eq 1a can be transformed into

$$d[Bi]/dt = k_{1,i}[E_0 i] - (k_{1,i} + k_{2,i})[Bi] \qquad \text{(2a)}$$

Upon integration of eq 2a and taking into account $[Bi] = 0$ at $t = 0$, $[Bi]$ is expressed by

$$[Bi] = \frac{k_{1,i}[E_0 i]}{k_{1,i} + k_{2,i}}[1 - e^{-(k_{1,i}+k_{2,i})t}] \qquad \text{(3a)}$$

The concentration of free radioactive aminoacyl-tRNA as a function of time is expressed by eq 4a, obtained by integrating

$$[Ri] = \int_0^t k_{2,i}[Bi] = \frac{k_{1,i}k_{2,i}}{k_{1,i} + k_{2,i}}[E_0 i]\left[t + \frac{e^{-(k_{1,i}+k_{2,i})t} - 1}{k_{1,i} + k_{2,i}} \right] \qquad \text{(4a)}$$

the rate equation $d[Ri]/dt = k_{2,i}[Bi]$, and considering $[Ri] = 0$ at $t = 0$. The expression of the total concentration of aminoacyl-tRNA for the ith site is given by the sum $[Bi] + [Ri]$ = eq 3a + eq 4a.

For model A, in the case of labeled preformed adenylates, the concentration of total labeled aminoacyl-tRNA as a function of time is

$$[R_T] = \sum_{i=1}^{i=2}[R_T i] \quad (5a)$$

for which the final expression is eq 1 given in the text. For models B–D, in the case of radioactive preformed adenylates, the concentration of R_T as a function of time is expressed by the same equation (4a), making $k_{1,2}$ and $k_{2,2} = 0$. Therefore, detailed calculations are not presented.

In the case of nonradioactive preformed adenylates, the simplified scheme (II) can be considered. As in the former

$$Ai \xrightarrow{k_{1,i}} Bi \xrightarrow{k_{2,i}} Ci \xrightarrow{k_{1,i}} Di \xrightarrow{k_{2,i}} Ci + Ri \quad (II)$$

case, only one site will be considered. The total radioactive aminoacyl-tRNA concentration for the ith site is $[R_T i] = [Di] + [Ri]$. The rate equations for free and bound aminoacyl-tRNA are eq 6a and 7a, respectively; then, the rate equation for $[R_T i]$ is eq 8a. The rate equations for $[Ai]$ and $[Ci]$ and the conservation equation are expressed as follows:

$$d[Ri]/dt = k_{2,i}[Di] \quad (6a)$$

$$d[Di]/dt = k_{1,i}[Ci] - k_{2,i}[Di] \quad (7a)$$

$$d[R_T i]/dt = k_{1,i}[Ci] \quad (8a)$$

$$d[Ai]/dt = -k_{1,i}[Ai] \quad (9a)$$

$$d[Ci]/dt = k_{2,i}([Bi] + [Di]) - k_{1,i}[Ci] \quad (10a)$$

$$[E_0 i] = [Ai] + [Bi] + [Ci] + [Di] \quad (11a)$$

Integrating eq 9a and considering $[Ai] = [E_0 i]$ at $t = 0$, one obtains

$$[Ai] = [E_0 i]e^{-k_{1,i}t} \quad (12a)$$

Using the value of $[Bi] + [Di]$ in eq 11a and the value of $[Ai]$ in eq 12a, eq 10a can be transformed into

$$d[Ci]/dt + (k_{1,i} + k_{2,i})[Ci] = k_{2,i}[E_0 i](1 - e^{-k_{1,i}t}) \quad (13a)$$

This linear first-order differential equation can be integrated as follows: Integration of the first member of the equation gives the general solution:

$$[Ci] = [C1]e^{-(k_{1,i}+k_{2,i})t} \quad (14a)$$

Derivation of eq 14a and replacing $d[Ci]/dt$ and $[Ci]$ by their values in eq 13a give

$$d[C1]/dt = k_{2,i}[E_0 i][e^{(k_{1,i}+k_{2,i})t} - e^{k_{2,i}t}] \quad (15a)$$

Integration of eq 15a and considering $[C1] = 0$ at $t = 0$ give

$$[C1] = k_{2,i}[E_0 i]\left[\frac{[e^{(k_{1,i}+k_{2,i})t} - 1]}{k_{1,i} + k_{2,i}} - \frac{e^{k_{2,i}t} - 1}{k_{2,i}}\right] \quad (16a)$$

Replacing $[C1]$ by its value in eq 14a gives the expression of $[Ci]$ as a function of time:

$$[Ci] = [E_0 i]\left[\frac{k_{2,i}}{k_{1,i} + k_{2,i}} - e^{-k_{1,i}t} + \frac{k_{1,i}}{k_{1,i} + k_{2,i}}e^{-(k_{1,i}+k_{2,i})t}\right] \quad (17a)$$

The concentration of radioactive aminoacyl-tRNA for the ith site, as a function of time, is obtained by integrating the rate equation (8a), taking the value of $[Ci]$ in eq 17a and considering $[R_T i] = 0$ at $t = 0$.

The concentration of total radioactive aminoacyl-tRNA as a function of time considering both sites is given by eq 2, given in the text, and is obtained by

$$[R_T] = \sum_{i=1}^{i=2}[R_T i]$$

Model B. The analytical expressions are obtained as above by considering only one functional site ($i = 1$). In this case, $k_{1,2}$ and $k_{2,2}$ are equal to 0.

Model C. In the case of nonradioactive preformed adenylates, Scheme VI can be written in a simpler form as

$$A \xrightarrow{k_1} B \xrightarrow{k_2} C \xrightarrow{k_1} D \xrightarrow{k_2} E \xrightarrow{k_1} F \xrightarrow{k_2} E + R \quad (VI)$$

The total radioactive aminoacyl-tRNA concentration is $[R_T] = [F] + [R]$; the rate equations for free and bound radioactive aminoacyl-tRNA are eq 1c and 2c, respectively; then, the rate equation for $[R_T]$ is eq 3c. The principle of the calculation is to determine, step by step, the expressions of the concentration of complexes A, B, C, and E as a function of time. The rate equations and the conservation equation are expressed as

$$d[R]/dt = k_2[F] \quad (1c)$$

$$d[F]/dt = k_1[E] - k_2[F] \quad (2c)$$

$$d[R_T]/dt = k_1[E] \quad (3c)$$

$$d[A]/dt = -k_1[A] \quad (4c)$$

$$d[B]/dt = k_1[A] - k_2[B] \quad (5c)$$

$$d[C]/dt = k_2[B] - k_1[C] \quad (6c)$$

$$d[E]/dt = k_2([D] + [F]) - k_1[E] \quad (7c)$$

$$[E_0] = [A] + [B] + [C] + [D] + [E] + [F] \quad (8c)$$

Integration of eq 4c, taking $[A] = [E_0]$ at $t = 0$, gives

$$[A] = [E_0]e^{-k_1 t} \quad (9c)$$

When $[A]$ is replaced by its value, eq 5c is transformed into a linear first-order differential equation, which can be integrated as above to give

$$[B] = \frac{k_1[E_0]}{k_2 - k_1}(e^{-k_1 t} - e^{-k_2 t}) \quad (10c)$$

In a similar way, eq 6c is transformed into a first-order differential equation by using the value of $[B]$ in eq 10c. Integration of this equation leads to

$$[C] = -\frac{k_1 k_2[E_0]}{k_1 - k_2}\left[te^{-k_1 t} + \frac{e^{-k_1 t}}{k_1 - k_2} + \frac{e^{-k_2 t}}{k_2 - k_1}\right] \quad (11c)$$

The rate equation (12c) is obtained from eq 7c by replacing $[D] + [F]$ by its value in the conservation equation (8c). By use of the expressions of $[A]$, $[B]$, and $[C]$ as a function of time (eq 9c, 10c, and 11c, respectively), the linear first-order equation (12c) can be integrated as above, considering $[E] = 0$ when $t = 0$, to give eq 13c. The concentration of total radioactive aminoacyl-tRNA as a function of time (eq 5 in the text) is obtained by integration of the rate equation (3c), taking the value of $[E]$ in eq 13c and considering $[R_T] = 0$ at $t = 0$.

$$d[E]/dt = k_2[E_0] - (k_1 + k_2)[E] - k_2([A] + [B] + [C]) \quad (12c)$$

$$[E] = \frac{k_1[E_0]}{k_1 + k_2}e^{-(k_1+k_2)t} + \frac{k_1 k_2 - (k_2 - k_1)^2}{(k_1 - k_2)^2}[E_0]e^{-k_1 t} - \frac{[E_0]k_1 k_2 e^{-k_2 t}}{(k_1 - k_2)^2} + \frac{k_2[E_0]}{k_1 + k_2} - \frac{k_1 k_2[E_0]te^{-k_1 t}}{k_2 - k_1} \quad (13c)$$

Model D. This model can be depicted, in the case of non-radioactive preformed adenylates, by a simplified form of the Scheme VIII:

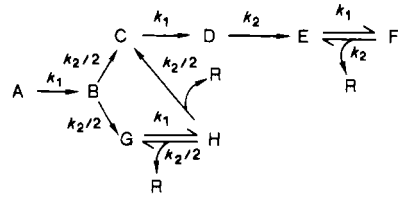

The total radioactive aminoacyl-tRNA concentration is $[R_T] = [R] + [F] + [H]$. The rate equations for free and bound aminoacyl-tRNA are eq 1d and 2d, respectively; then, the rate equation for $[R_T]$ is eq 3d. The rate and the conservation equations are expressed as

$$d[R]/dt = k_2([F] + [H]) \quad (1d)$$

$$d([F] + [H])/dt = k_1([G] + [E]) - k_2([H] + [F]) \quad (2d)$$

$$d[R_T]/dt = k_1([G] + [E]) \quad (3d)$$

$$d[A]/dt = -k_1[A] \quad (4d)$$

$$d[B]/dt = k_1[A] - k_2[B] \quad (5d)$$

$$d[C]/dt = (k_2/2)([B] + [H]) - k_1[C] \quad (6d)$$

$$d[D]/dt = k_1[C] - k_2[D] \quad (7d)$$

$$d[E]/dt = k_2([D] + [F]) - k_1[E] \quad (8d)$$

$$d[F]/dt = k_1[E] - k_2[F] \quad (9d)$$

$$d[G]/dt = (k_2/2)([B] + [H]) - k_1[G] \quad (10d)$$

$$d[H]/dt = k_1[G] - k_2[H] \quad (11d)$$

$$[E_0] = [A] + [B] + [C] + [D] + [E] + [F] + [G] + [H] \quad (12d)$$

Integration of eq 4d and 5d, considering $[A] = [E_0]$ and $[B] = 0$ at $t = 0$, gives

$$[A] = [E_0]e^{-k_1t} \quad (13d)$$

$$[B] = \frac{k_1[E_0]}{k_2 - k_1}(e^{-k_1t} - e^{-k_2t}) \quad (14d)$$

Upon derivation of eq 10d, one obtains

$$d^2[G]/dt^2 = (k_2/2)(d[B]/dt) + (k_2/2)(d[H]/dt) - k_1(d[G]/dt) \quad (15d)$$

By replacing $d[H]/dt$ in eq 15d by its value in eq 11d, one obtains

$$d^2[G]/dt^2 = (k_2/2)(d[B]/dt) + (k_1k_2/2)[G] - (k_2^2/2)[H] - k_1(d[G]/dt) \quad (16d)$$

By replacing [H] in eq 16d by its value in eq 10d, one obtains

$$(d^2[G]/dt^2) + (k_1 + k_2)(d[G]/dt) + (k_1k_2/2)[G] = (k_2/2)[(d[B]/dt) + k_2[B]] \quad (17d)$$

By replacing $d[B]/dt$ and [B] in eq 17d by their values derived from eq 14d, one obtains

$$(d^2[G]/dt^2) + (k_1 + k_2)(d[G]/dt) + (k_1k_2/2)[G] = (k_1k_2/2)[E_0]e^{-k_1t} \quad (18d)$$

This second-order differential equation was integrated as follows: The general solution of eq 18d without second member is expressed by

$$[G]_g = [C1]e^{r_1t} + [C2]e^{r_2t} \quad (19d)$$

$$r_1 = (-k_1 - k_2 + V)/2 \qquad r_2 = (-k_1 - k_2 - V)/2$$
$$V = (k_1^2 + k_2^2)^{1/2}$$

A particular solution of eq 18d is $[Y] = -[E_0]e^{-k_1t}$; then, the solution of eq 18d is

$$[G] = [G]_g + [Y] = [C1]e^{r_1t} + [C2]e^{r_2t} - [E_0]e^{-k_1t} \quad (20d)$$

Taking into account $[G] = 0$ and $d[G]/dt = 0$ at $t = 0$, [C1] and [C2] can be calculated:

$$[C1] = \frac{[E_0](r_2 + k_1)}{r_2 - r_1} \quad (21d)$$

$$[C2] = -\frac{[E_0](r_1 + k_1)}{r_2 - r_1} \quad (22d)$$

Then eq 20d can be transformed into

$$[G] = [E_0]\left[-\frac{k_1 - k_2 - V}{2V}e^{r_1t} + \frac{k_1 - k_2 + V}{2V}e^{r_2t} - e^{-k_1t}\right] \quad (23d)$$

Concentrations of complexes H, G, and D as functions of time can be calculated by using eq 11d, 6d, and 7d and values of [A], [B], and [G] in eq 13d, 14d, and 23d:

$$[H] = \frac{k_1[E_0]}{V}(e^{r_1t} - e^{r_2t}) + \frac{k_1[E_0]}{k_2 - k_1}(e^{-k_2t} - e^{-k_1t}) \quad (24d)$$

$$[C] = \frac{-[E_0]}{2V}[(k_1 - k_2 - V)e^{r_1t} - (k_1 - k_2 + V)e^{r_2t} + 2Ve^{-k_1t}] \quad (25d)$$

$$[D] = \frac{k_1[E_0]}{V}\left[e^{r_1t} - e^{r_2t} - \frac{V}{k_2 - k_1}(e^{-k_1t} - e^{-k_2t})\right] \quad (26d)$$

Concentration of complex F as a function of time can be calculated by integration of eq 9d, using the value of [E] from the conservation equation (12d) and the value of [A], [B], [C], [D], [G], and [H] in eq 13d, 14d, 25d, 26d, 23d, and 24d, respectively, and considering $[F] = 0$ at $t = 0$.

$$[F] = \frac{k_1}{k_1 + k_2}[E_0][1 - e^{-(k_1+k_2)t}] + \frac{k_1}{k_2 - k_1}[E_0](e^{-k_1t} - e^{-k_2t}) - \frac{2k_1}{V}[E_0](e^{r_1t} - e^{r_2t}) \quad (27d)$$

The radioactive aminoacyl-tRNA concentration can be calculated by integration of eq 3d, using the value of [E] from the conservation equation (12d) and the analytical expression of the other complexes as described above. The value of $[R_T]$ as a function of time is given in the text by eq 6.

Registry No. L-Trp, 73-22-3; tryptophanyl adenylate, 31528-64-0; tryptophanyl-tRNA synthetase, 9023-44-3.

References

Akhverdyan, V. Z., Kisselev, L. L., Knorre, D. G., Lavrik, O. I., & Nevinsky, G. A. (1977) *J. Mol. Biol. 113*, 475–501.

Bale, J. R., Chock, P. B., & Huang, C. Y. (1980a) *J. Biol. Chem. 255*, 8424–8430.

Bale, J. R., Chock, P. B., & Huang, C. Y. (1980b) *J. Biol. Chem. 255*, 8431–8436.

Cleland, W. W. (1963) *Biochim. Biophys. Acta 67*, 104–196.

Cornish-Bowden, A., & Wong, J. T. (1978) *Biochem. J. 175*, 969–976.

Dorizzi, M., Mérault, G., Fournier, M., Labouesse, J., Keith, G., Dirheimer, G., & Buckingham, R. (1977) *Nucleic Acids Res. 4*, 31-41.
Fasiolo, F., Ebel, J. P., & Lazdunski, M. (1977) *Eur. J. Biochem. 73*, 7-15.
Favorova, O. O., Madoyan, I. A., & Drusta, V. L. (1981) *FEBS Lett. 123*, 161-165.
Fournier, M., Dorizzi, M., Sarger, C., & Labouesse, J. (1976) *Biochimie 58*, 1159-1165.
Freist, W., & Cramer, E. (1983) *Eur. J. Biochem. 131*, 65-80.
Gangloff, J., Pouyet, J., & Dirheimer, G. (1984) *J. Biochem. Biophys. Methods 9*, 201-213.
Graves, P. V., Mazat, J. P., Juguelin, H., Labouesse, J., & Labouesse, B. (1979) *Eur. J. Biochem. 96*, 509-518.
Graves, P. V., de Bony, J., Mazat, J. P., & Labouesse, B. (1980) *Biochimie 62*, 33-41.
Hammes, G. G., & Schimmel, P. R. (1970) *Enzymes (3rd Ed.) 2*, 67-114.
Huang, C. Y., Rhee, S. G., & Chock, P. B. (1982) *Annu. Rev. Biochem. 51*, 935-971.
Iborra, F., Dorizzi, M., & Labouesse, J. (1973) *Eur. J. Biochem. 39*, 275-282.
Jakes, R., & Fersht, A. R. (1975) *Biochemistry 14*, 3344-3350.
Kern, D., & Lapointe, J. (1981) *Eur. J. Biochem. 115*, 29-38.
Lazdunski, M. (1972) *Curr. Top. Cell. Regul. 6*, 267-310.
Lemaire, G., Van Rapenbush, R., Gros, C., & Labouesse, B. (1969) *Eur. J. Biochem. 10*, 336-344.
Mazat, J. P., Merle, M., Graves, P. V., Mérault, G., Gandar, J. C., & Labouesse, B. (1982) *Eur. J. Biochem. 128*, 389-398.
Mehler, A., & Chakraburty, K. (1971) *Adv. Enzymol. Relat. Areas Mol. Biol. 35*, 443-501.
Mérault, G., Graves, P. V., Labouesse, B., & Labouesse, J. (1978) *Eur. J. Biochem. 87*, 541-550.
Merle, M., Graves, P. V., & Labouesse, B. (1984) *Biochemistry 23*, 1716-1723.
Mulvey, R. S., & Fersht, A. R. (1978) *Biochemistry 17*, 5591-5597.
Nishimura, S., & Novelli, G. D. (1964) *Biochim. Biophys. Acta 80*, 574-586.
O'Sullivan, W. J., & Smithers, G. W. (1979) *Methods Enzymol. 63*, 294-336.
Pachmann, U., & Zachau, H. G. (1978) *Nucleic Acids Res. 5*, 961-973.
Penneys, N. S., & Muench, K. H. (1974) *Biochemistry 13*, 566-571.
Pingoud, A., Boehme, D., Riesner, D., Kuwnatski, R., & Maass, G. (1975) *Eur. J. Biochem. 56*, 617-622.
Schimmel, P. R., & Söll, D. (1979) *Annu. Rev. Biochem. 48*, 601-648.
Thiebe, R. (1978) *Nucleic Acids Res. 6*, 2055-2071.
Thiebe, R. (1983) *Eur. J. Biochem. 130*, 517-524.
Trézéguet, V., Merle, M., Gandar, J. C., & Labouesse, B. (1983) *FEBS Lett. 157*, 210-214.
Weiss, S. B., Zachau, H. G., & Lipmann, F. (1959) *Arch. Biochem. Biophys. 83*, 101-105.
Zinoviev, V. V., Rubtsova, N. G., Lavrik, O. I., Malygin, E. G., Akhverdyan, V. Z., Favorova, O. O., & Kisselev, L. L. (1977) *FEBS Lett. 82*, 130-134.

Kinetics of Slow, Tight-Binding Inhibitors of Angiotensin Converting Enzyme†

Umesh B. Goli* and Richard E. Galardy
Department of Biochemistry and Sanders-Brown Research Center on Aging, University of Kentucky, Lexington, Kentucky 40536

Received March 19, 1986; Revised Manuscript Received June 26, 1986

ABSTRACT: Five phosphorus-containing inhibitors of angiotensin converting enzyme were found to exhibit slow, tight-binding kinetics by using furanacryloyl-L-phenylalanylglycylglycine as substrate at pH 7.50 and $T = 25$ °C. Two of the inhibitors, (*O*-ethylphospho)-Ala-Pro (**2**) and (*O*-isopropylphospho)-Ala-Pro (**3**), are found to follow at minimum a two-step mechanism of binding (mechanism B) to the enzyme. This mechanism consists of an initial fast formation of a weaker enzyme–inhibitor complex (K_i = 130 nM for **2** and 180 nM for **3**) followed by a slow reversible isomerization to a tighter complex with measurable forward (k_3) and reverse (k_4) rate constants ($k_3 = 4.5 \times 10^{-2}$ s^{-1} for **2** and 5.4×10^{-2} s^{-1} for **3**; $k_4 = 9.2 \times 10^{-3}$ s^{-1} for **2** and 3.5×10^{-3} s^{-1} for **3**). For the remaining three inhibitors, phospho-Ala-Pro (**1**), (*O*-benzylphospho)-Ala-Pro (**4**), and (*P*-phenethylphosphono)-Ala-Pro (**5**), a one-step binding mechanism (mechanism A) is observed under the conditions of the experiment. The second-order rate constants k_1 (M^{-1} s^{-1}) for the binding of these inhibitors to converting enzyme are found to have values more than 3 orders of magnitude lower than the diffusion-controlled limit for a bimolecular reaction involving the enzyme, viz., 3.9×10^5 for **1**, 2.2×10^5 for **4**, and 4.8×10^5 for **5**. The rate constants, k_2, for the dissociation of the enzyme–inhibitor complexes following this mechanism are 5.1×10^{-3} s^{-1} for **1**, 2.0×10^{-3} s^{-1} for **4**, and 5.3×10^{-5} s^{-1} for **5**. The overall dissociation constants for these inhibitors as determined from Henderson plots are 13 nM for **1**, 22 nM for **2**, 11 nM for **3**, 9.2 nM for **4**, and 0.11 nM for **5**.

The reversible, slow, tight-binding inhibition of enzymes has been reviewed recently (Williams & Morrison, 1979; Morrison, 1982). A reversible, tight-binding inhibitor is one that reversibly inhibits the enzyme-catalyzed reaction at concentrations comparable to that of the enzyme either due to low K_i value or due to high concentrations of enzyme necessary for low turnover number enzyme–substrate systems or due to both. The classical Michaelis–Menten equation cannot be used to determine the potency of such inhibitors because an assumption is made in the derivation of this equation that the depletion

† This study was supported by NIH Grant HL 27368.

0006-2960/86/0425-7136$01.50/0